

Supporting Information

Glycocalixarene with Luminescence for Warburg Effect-mediated Tumor

Imaging and Targeted Drug Delivery

Yang Li ^{a, #}, Shengnan Liu ^{b, #}, Min Liang ^c, Yujun Cui ^d, Hongxia Zhao^{*, a} and Qingzhi Gao^{*, a}

^a Tianjin Key Laboratory for Modern Drug Delivery & High-Efficiency, School of Pharmaceutical Science and Technology, Tianjin University, 92 Weijin Road, Nankai District, Tianjin 300072, P. R. China.

^b Institute of Molecular Plus, School of Chemical Engineering and Technology, Tianjin University, 92 Weijin Road, Nankai District, Tianjin 300072, P. R. China.

^c Central Institute of Pharmaceutical Research, CSPC Pharmaceutical Group, 226 Huanghe Road, Shijiazhuang, Hebei, 050035, P. R. China.

^d Transplantation Center, Tianjin First Central Hospital, 24 Fukang Road, Nankai District, Tianjin 300192, P. R. China.

These authors contributed equally to this work.

*Corresponding Authors:

Hongxia Zhao* E-mail: zhaohongxia@tju.edu.cn

Qingzhi Gao* E-mail: qingzhi@tju.edu.cn

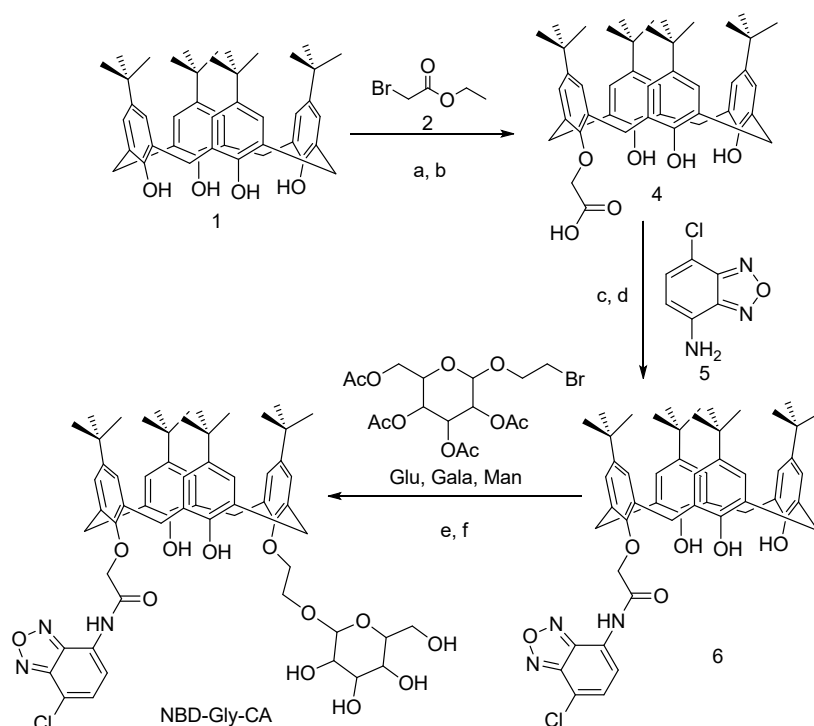
Table of Contents

1. General	S1
2. Chemistry	S1-S4
Scheme S1: Synthesis of NBD-Gly-CA.	
3. Analytical Data of the Compounds	S4-S10
Figure S1: ¹ H-NMR spectrum of compound 4	
Figure S2: ¹ H-NMR spectrum of compound 7	
Figure S3. ¹ H-NMR spectrum of NBD-Glu-CA	
Figure S4. ¹³ C-NMR spectrum of NBD-Glu-CA	
Figure S5. IR spectrum of NBD-Glu-CA	
Figure S6. ¹ H-NMR spectrum of NBD-Man-CA	
Figure S7. ¹³ C-NMR spectrum of NBD-Man-CA	
Figure S8. IR spectrum of NBD-Man-CA	
Figure S9. ¹ H-NMR spectrum of NBD-Gala-CA	
Figure S10. ¹³ C-NMR spectrum of NBD-Gala-CA	
Figure S11. IR spectrum of NBD-Gala-CA	
Figure S12. HRMS spectrum of NBD-Gala-CA	
4. Photophysical Properties of the Probes	S10-S11
Figure S13: Fluorescent spectrum of NBD-Gly-CA	
5. Biological Experimental Procedures	S11-S12
Cell lines and cell culture	
Cell Viability Assay	
NBD-Gly-CA accumulation in different cell lines.	
ATP-mediated glucose uptake inhibition	
Confocal Fluorescence Imaging	
<i>In Vivo</i> Fluorescence Imaging of NBD-Man-CA in MDA-MB-468 Xenograft Mice.	
6. Biological Assay Results	S13-S16
Figure S14. NBD-Gly-CA accumulation in different cell lines	
Figure S15. Confocal fluorescence microscopy imaging of NBD-Man-CA in different cell lines	
Figure S16: <i>In vivo</i> imaging for NBD-Man-CA treated A549 xenograft mice	
Table S1: Tumor-to-background ration (Tm/Bkg) and tumot-to-organ ratio (Tm/Org) for NBD-Man-CA treated MDA-MB-468 bearing xenograft mice	
Figure S17. Molecular dynamics simulations of NBD-Gly-CA with different drug molecules	
Figure S18. <i>In vitro</i> cytotoxicities of DDP⊂NBD-Man-CA against A549, BEAS-2B, MDA-MB-468 and MCF-10A cells	
Figure S19. Cytotoxicity of NBD-Gly-CA in A549 and MDA-MB-468 cells	
Figure S20 UV-vis based binding constant analysis and interaction map for DDP⊂NBD-Man-CA	

1. General

Materials and Instrumentation. For chemistry, all chemicals were obtained from commercial suppliers and were used as received. If necessary, the reactions were carried out in dry solvents and under an argon atmosphere. ^1H and ^{13}C NMR spectra were recorded with a Bruker Avance 400 or 600 MHz at the School of Pharmaceutical Science and Technology of Tianjin University, PRC. Data are reported as chemical shifts (δ) in parts per million (ppm) relative to the solvent peak, and scalar coupling constants (J) are reported in units of hertz (Hz). Infrared spectra were recorded using a Bruker Tensor II FT-IR spectrometer. Absorptions are reported in wavenumbers (cm^{-1}). Absorptions are reported in wavenumbers (cm^{-1}). UV-visible spectroscopic analysis was performed using a U-3900 UV-VIS spectrophotometer at room temperature with a quartz cuvette having a pathlength of 0.2 cm as a sample holder. Fluorescence spectra were measured using a Varioskan LUX multimode microplate reader (Thermo Fisher Scientific). High-resolution mass spectra (HRMS, m/z) were recorded on a Thermo Scientific™ Q Exactive™ HF spectrometer in positive mode (ESI^+).

2. Chemistry



Scheme S1. Synthesis of NBD-Gly-CA: a) CsF, DMF, 80 °C; b) NaOH, EtOH, H₂O, reflux; c) SOCl₂, d) pyridine, CH₂Cl₂; e) KI, K₂CO₃, CH₃CN, 80 °C; f) NaOH, MeOH, H₂O;

5,11,17,23-tetra-tert-butyl-25-ethoxycarbonylmethoxy-26,27,28-trihydroxycalix[4]arene (3). A mixture of Compound 1 (500 mg, 0.77 mmol), ethyl bromoacetate (170 μL , 1.54 mmol), CsF (140 mg 0.92 mmol) and DMF (10 ml) was stirred at 80 °C for 16 h. The reaction mixture was cooled to room temperature, then a Et₂O (300 ml) and H₂O (150 ml), then the

combined organic phases were washed with water and evaporated in vacuum. The crude was purified by column chromatography on silica gel with EtOAc/hexane to get a white solid (328mg, 58%). ¹H NMR (600 MHz, CDCl₃) δ 7.02 (s, 4H, ArH), 6.81 (s, 4H, ArH), 4.72 (s, 2H, OCH₂), 4.45 (d, *J* = 13.2 Hz, 4H, ArCH₂Ar), 4.30 (q, *J* = 7.1 Hz, 2H, CH₂CH₃), 3.32 (d, *J* = 13.2 Hz, 4H, ArCH₂Ar), 1.34 (t, *J* = 7.1 Hz, 3H, CH₂CH₃), 1.26 (s, 18H, C(CH₃)₃), 0.97 (s, 18H, C(CH₃)₃).

5,11,17,23-tetra-tert-butyl-25-(carboxymethoxy)-26,27,28-trihydroxycalix[4]arene (4).

Compound 3 (328 mg, 0.44 mmol) was dissolved in EtOH (9 ml), a solution of NaOH (89 mg, 2.2 mmol) and H₂O (6 ml) was added, the mixture was reflux for 4h, The reaction mixture was evaporated to remove solvent. 5% HCl was added until pH 1. The resulting product was filtered, and get the compound 4 (300 mg, 95.2%). ¹H NMR (400 MHz, DMSO-*d*₆) δ 14.72 (s, 2H, COOH, ArOH), 7.08 (d, *J* = 2.3 Hz, 2H, ArH), 6.90 (s, 2H, ArH), 6.86 – 6.74 (m, 4H, ArH), 4.32 (d, *J* = 11.8 Hz, 2H, ArCH₂Ar), 4.08 (d, *J* = 12.5 Hz, 2H, ArCH₂Ar), 3.74 (s, 2H, OCH₂), 3.14 (d, *J* = 12.2 Hz, 4H, ArCH₂Ar), 1.16 (d, *J* = 13.7 Hz, 27H, C(CH₃)₃), 1.04 (s, 9H, C(CH₃)₃).

5,11,17,23-tetra-tert-butyl-25-((7-chloro-2,1,3-benzoxadiazole-4-yl)carbamoylmethoxy)-26,27,28-trihydroxycalix[4]arene (7). A solution of compound 4 (100 mg, 0.14 mmol) and SOCl₂ (410 μL) was heated at reflux. After 4 h, the SOCl₂ was removed under reduced pressure. The crude added to the reaction mixture of compound 6 (166 mg, 0.15 mmol), pyridine (12 μL, 0.15mmol) and anhydrous CH₂Cl₂. Stirred at room temperature for overnight. Then the reaction mixture was evaporated to remove solvent. The solid was added Et₂O (10 mL), washed by water (10 ml) and brine (10 ml). The organic layer was dried over Na₂SO₄ and the solvents were removed under vacuum. The crude product was purified by silica gel column chromatography using petroleum ether–ethylacetate to give compound 7 (60 mg, 49%) as yellow solid. ¹H NMR (600 MHz, CDCl₃) δ 11.22 (s, 1H, CONH), 9.77 (s, 1H, ArOH), 9.21 (s, 2H, ArOH), 8.25 (d, *J* = 7.8 Hz, 1H, ArH), 7.47 (d, *J* = 7.8 Hz, 1H, ArH), 7.08 (d, *J* = 3.5 Hz, 6H, ArH), 7.04 (d, *J* = 2.1 Hz, 2H, ArH), 4.80 (s, 2H, OCH₂), 4.36 (d, *J* = 13.9 Hz, 2H, ArCH₂Ar), 4.22 (d, *J* = 13.3 Hz, 2H, ArCH₂Ar), 3.51 (t, *J* = 13.0 Hz, 4H, ArCH₂Ar), 1.22-1.23 (m, 27H, C(CH₃)₃), 1.17 (s, 9H, C(CH₃)₃).

NBD-AcGlc-CA (8). Added the catalytic amount of KI to the solution of 2-bromoethyl-2,3,4,6-tetra-O-acetyl-β-D-glucopyranoside (187 mg, 0.15 mmol) and anhydrous CH₃CN (10 ml), stirred at 80 °C for 30 min. Then add compound 7 (300mg, 0.13mmol) and K₂CO₃ (58mg, 0.13mmol). The mixture was stirred for 48 h. Then removed the solvent and dissolved in Et₂O (100 ml), washed with H₂O (50 ml) and brine (50 ml) and then dried. The solvent was removed under reduced pressure, and used ethyl acetate/pet.ether as eluting medium to purified the residue by silica gel column chromatography. Get the product (200mg, 46%) as yellow solid.

NBD-Glc-CA (9). Then the product (200 mg, 0.19 mmol) was dissolved in CH₃OH, cooled the mixture to 0 °C. Added the solution of NaOH (32 mg, 0.95 mmol) and H₂O (2 ml), then heated the reaction mixture to reflux for 1 h. Cooled to the room temperature, diluted with Et₂O (100 ml), washed with H₂O (3×50ml) and brine (50 ml), used anhydrous Na₂SO₄ to dried the organic phase

and concentrated. A pure compound NBD-Glc-CA (80 mg, 43%) was get after column chromatography with CH₂Cl₂-MeOH as the eluent (20:1, v/v) as yellow solid. ¹H NMR (600 MHz, CDCl₃) δ 10.67 (s, 1H, CONH), 8.50 (d, *J* = 7.9 Hz, 1H, ArH), 7.68 (s, 1H, ArH), 7.48 (d, *J* = 7.9 Hz, 1H), 7.15 (d, *J* = 2.1 Hz, 1H), 7.08 (d, *J* = 5.3 Hz, 3H), 7.05 (d, *J* = 2.1 Hz, 1H), 6.93 (s, 2H), 6.69 (d, *J* = 6.0 Hz, 2H), 4.90 (d, *J* = 15.4 Hz, 1H), 4.40 – 4.32 (m, 4H), 4.27 (t, *J* = 13.0 Hz, 3H), 4.16 (d, *J* = 10.4 Hz, 1H), 4.07 (dd, *J* = 10.4, 2.4 Hz, 1H), 3.85 (d, *J* = 7.6 Hz, 1H), 3.81 (dd, *J* = 11.9, 3.5 Hz, 1H), 3.72 (dd, *J* = 11.9, 4.7 Hz, 1H), 3.54 (d, *J* = 13.8 Hz, 1H), 3.49 – 3.44 (m, 2H), 3.35 – 3.26 (m, 3H), 3.21 (t, *J* = 9.1 Hz, 1H), 3.03 (dd, *J* = 9.0, 4.4 Hz, 1H), 1.29 (d, *J* = 13.4 Hz, 18H, C(CH₃)₃), 1.03 (s, 9H, C(CH₃)₃), 0.86 (s, 9H, C(CH₃)₃); ¹³C NMR (150 MHz, CDCl₃) δ 170.18 , 150.75 , 149.99 , 149.01 , 148.82 , 148.72 , 147.73 , 146.59 , 145.45 , 142.83 , 142.28 , 132.59 , 132.48 , 132.27 , 132.23 , 131.79 , 129.07 , 128.50 , 126.35 , 126.27 , 126.09 , 126.05 , 125.85 , 125.76 , 125.65 , 125.55 , 125.40 , 124.95 , 124.81 , 118.20 , 115.44 , 103.38 , 76.06 , 75.55 , 74.09 , 73.40 , 69.77 , 67.84 , 62.04 , 34.15 , 33.93 , 33.90 , 33.84 , 32.21 , 31.68 , 31.60 , 31.52 , 31.33 , 31.00 , 30.92 , 14.14; ESI-MS (*m/z*): calcd for C₆₀H₇₄ClN₃O₁₂ (M+Na)⁺: 1086.4961, found 1086.4856.

NBD-Man-CA (10). Compound 11 was synthesized according to compound 9 with the yield of 47%. ¹H NMR (600 MHz, CDCl₃) δ 10.79 (s, 1H, CONH), 8.42 (d, *J* = 7.9 Hz, 1H, ArH), 7.39 (d, *J* = 7.9 Hz, 1H, ArH), 7.08 (d, *J* = 3.4 Hz, 4H), 6.84 – 6.76 (m, 4H), 6.69 (d, *J* = 2.1 Hz, 2H), 4.91 (s, 1H), 4.73 (d, *J* = 15.6 Hz, 1H), 4.63 (d, *J* = 15.6 Hz, 1H), 4.37 (dd, *J* = 29.8, 13.6 Hz, 4H), 4.21 (dd, *J* = 24.2, 13.0 Hz, 2H), 4.04 (s, 1H), 3.89 (s, 1H), 3.82 – 3.64 (m, 4H), 3.55 (d, *J* = 8.4 Hz, 1H), 3.49 – 3.38 (m, 3H), 3.31 (dd, *J* = 25.1, 13.1 Hz, 2H), 1.29 (d, *J* = 2.6 Hz, 18H, C(CH₃)₃), 0.94 (s, 9H, C(CH₃)₃), 0.87 (s, 9H, C(CH₃)₃); ¹³C NMR (150 MHz, CDCl₃) δ 169.35 , 150.22 , 149.99 , 149.92 , 149.18 , 148.78 , 147.71 , 147.14 , 142.24 , 142.17 , 132.14 , 132.05 , 132.00 , 128.15 , 127.96 , 127.24 , 127.17 , 126.00 , 125.86 , 125.82 , 125.78 , 125.28 , 125.18 , 125.14 , 118.38 , 115.61 , 100.42 , 75.78 , 74.06 , 72.34 , 71.48 , 70.66 , 66.29 , 65.79 , 60.89 , 33.98 , 33.89 , 33.88 , 31.90 , 31.86 , 31.70 , 31.40 , 31.31 , 30.97 , 30.93 ; ESI-MS (*m/z*): calcd for C₆₀H₇₄ClN₃O₁₂ (M+Na)⁺: 1086.4961, found 1086.4856.

NBD-Gal-CA (11). Compound 10 was synthesized according to compound 9 with the yield of 35%. ¹H NMR (600 MHz, CDCl₃) δ 10.69 (s, 1H, CONH), 8.48 (d, *J* = 7.9 Hz, 1H, ArH), 7.72 (s, 1H), 7.46 (d, *J* = 7.9 Hz, 1H), 7.15 (d, *J* = 14.7 Hz, 2H), 7.08 (d, *J* = 5.3 Hz, 2H), 7.06 (s, 1H), 6.94 (d, *J* = 3.6 Hz, 2H), 6.69 (d, *J* = 15.0 Hz, 2H), 4.90 (d, *J* = 15.5 Hz, 1H), 4.35 (dd, *J* = 14.0, 8.5 Hz, 4H), 4.30 – 4.21 (m, 3H), 4.19 (s, 1H), 4.11 (d, *J* = 7.2 Hz, 1H), 3.86 (dd, *J* = 17.4, 8.6 Hz, 3H), 3.78 (dd, *J* = 11.8, 4.7 Hz, 1H), 3.63 – 3.57 (m, 1H), 3.54 (d, *J* = 13.9 Hz, 1H), 3.45 (d, *J* = 13.8 Hz, 1H), 3.34 – 3.25 (m, 3H), 3.24 – 3.15 (m, 1H), 1.30 (s, 9H, C(CH₃)₃), 1.28 (s, 9H, C(CH₃)₃), 1.03 (s, 9H, C(CH₃)₃), 0.86 (s, 9H, C(CH₃)₃); ¹³C NMR (150 MHz, CDCl₃) δ 171.18 , 170.16 , 169.49 , 150.88 , 150.70 , 149.96 , 148.95 , 148.84 , 148.80 , 147.64 , 146.53 , 145.46 , 142.85 , 142.33 , 132.56 , 132.50 , 132.21 , 132.12 , 131.69 , 129.08 , 128.58 , 127.20 , 126.40 , 126.34 , 126.31 , 126.04 , 126.02 , 125.86 , 125.76 , 125.73 , 125.71 , 125.65 , 125.55 , 125.52 , 125.48 , 125.03 , 124.92 ,

124.87 , 118.34 , 118.13 , 115.44 , 103.61 , 99.24 , 75.65 , 75.48 , 74.22 , 74.14 , 73.14 , 71.13 , 70.61 , 70.15 , , 68.88 , 67.58 , 66.29 , 62.50 , 62.21 , 62.09 , 60.42 , 53.27 , 34.15 , 34.13 , 34.07 , 33.95 , 33.89 , 33.82 , 32.88 , 32.20 , 32.05 , 31.69 , 30.91 , 29.70 , 21.00 , 14.13; ESI-MS (m/z): calcd for C₆₀H₇₄ClN₃O₁₂ (M+Na)⁺: 1086.4961, found 1086.4856.

3. Analytical Data of the Compounds

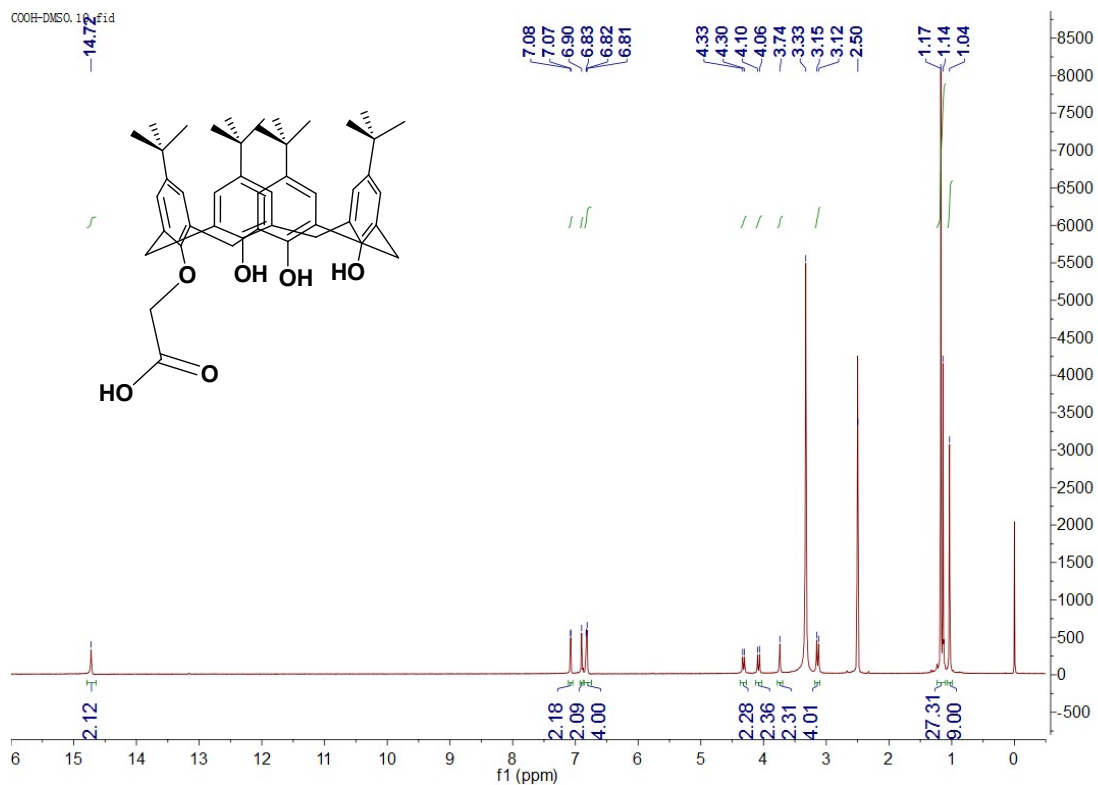


Figure S1. ¹H-NMR (600 MHz) spectrum of compound **4** in CDCl₃.

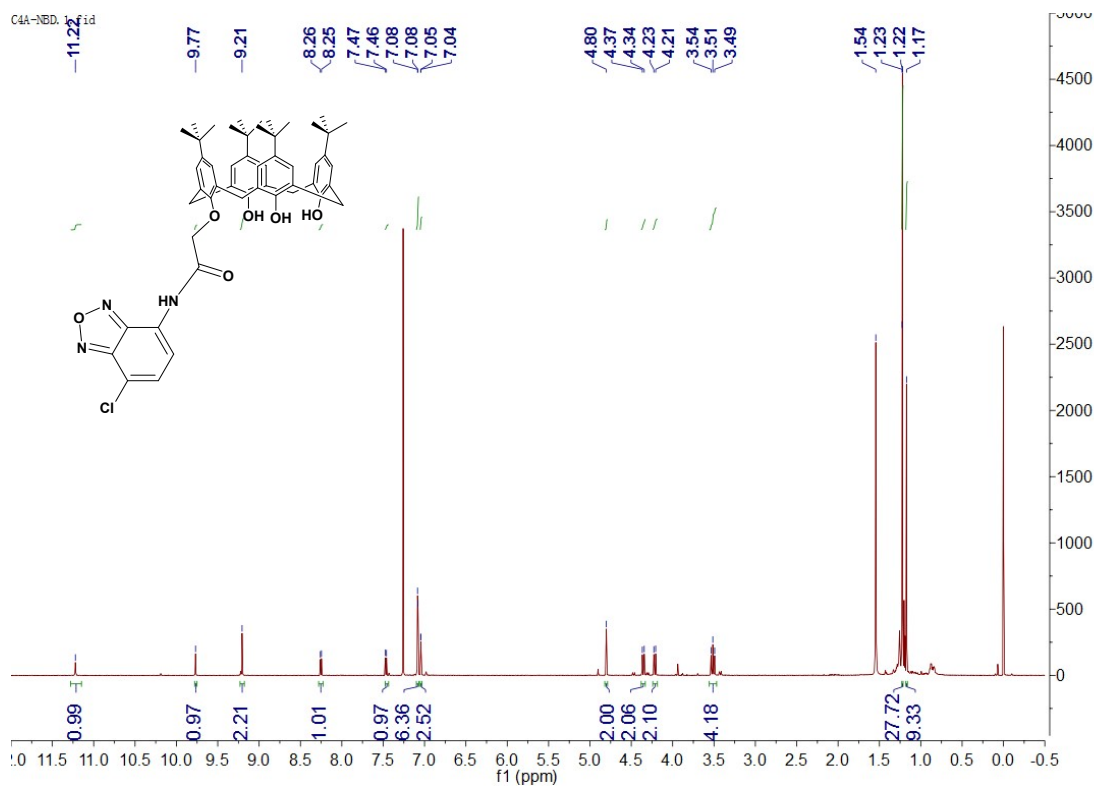


Figure S2. ¹H-NMR (600 MHz) spectrum of compound 7 in CDCl₃.

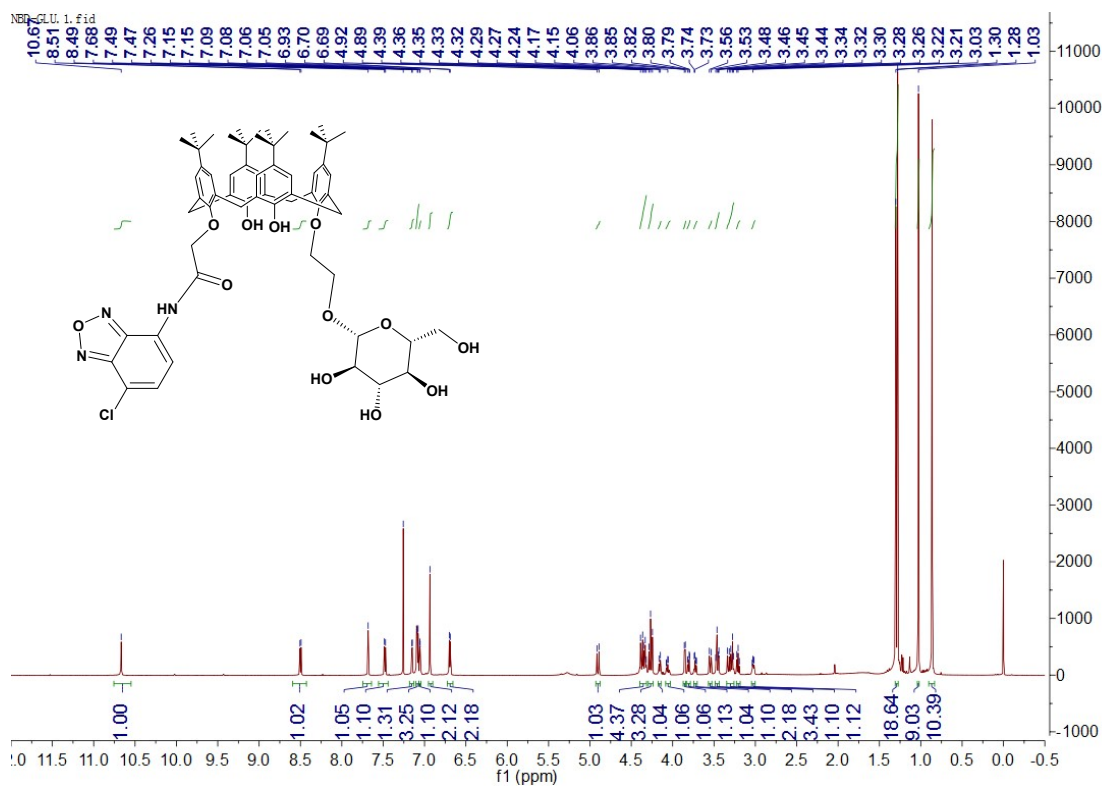


Figure S3. ¹H-NMR (600 MHz) spectrum of NBD-Glc-CA in CDCl₃.

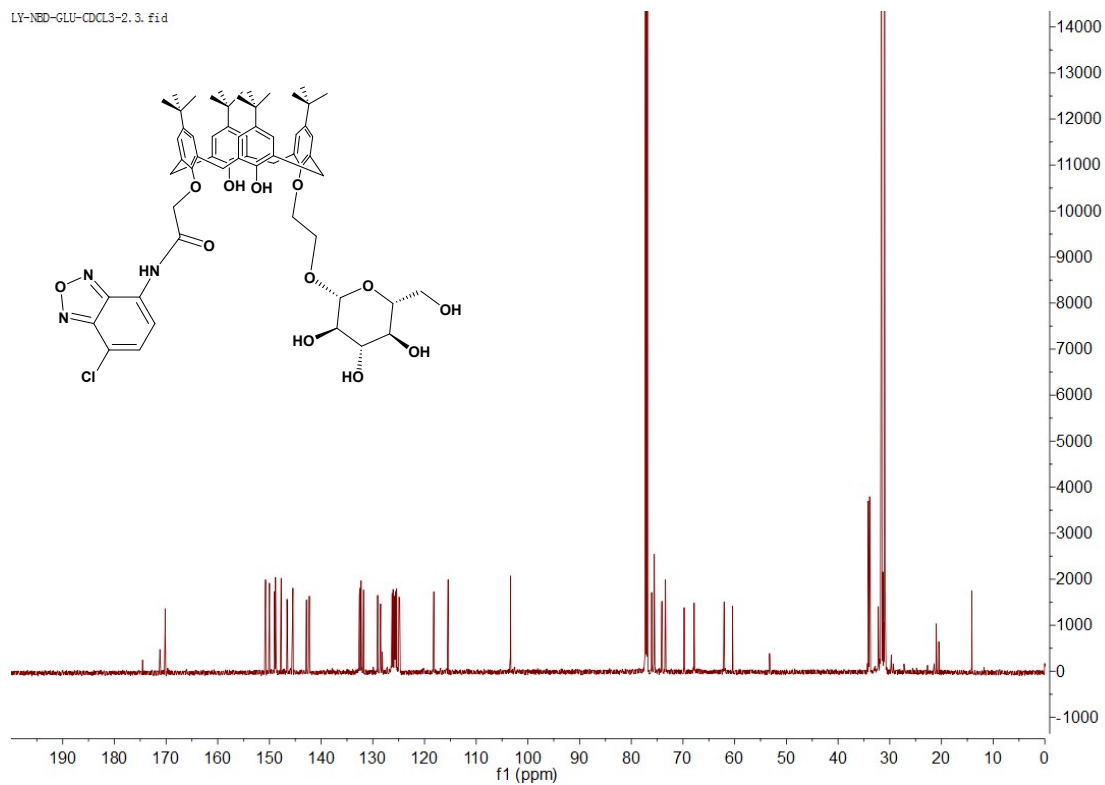


Figure S4. ^{13}C -NMR (150 MHz) spectrum of NBD-Glc-CA.

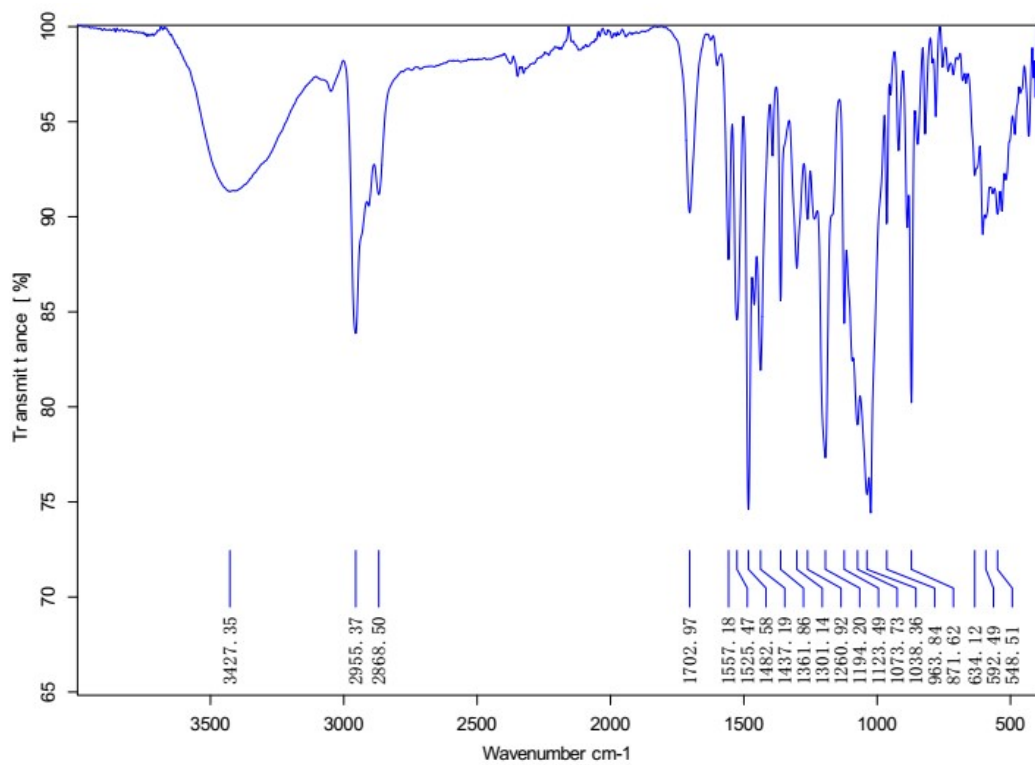


Figure S5. IR spectrum of NBD-Glc-CA.

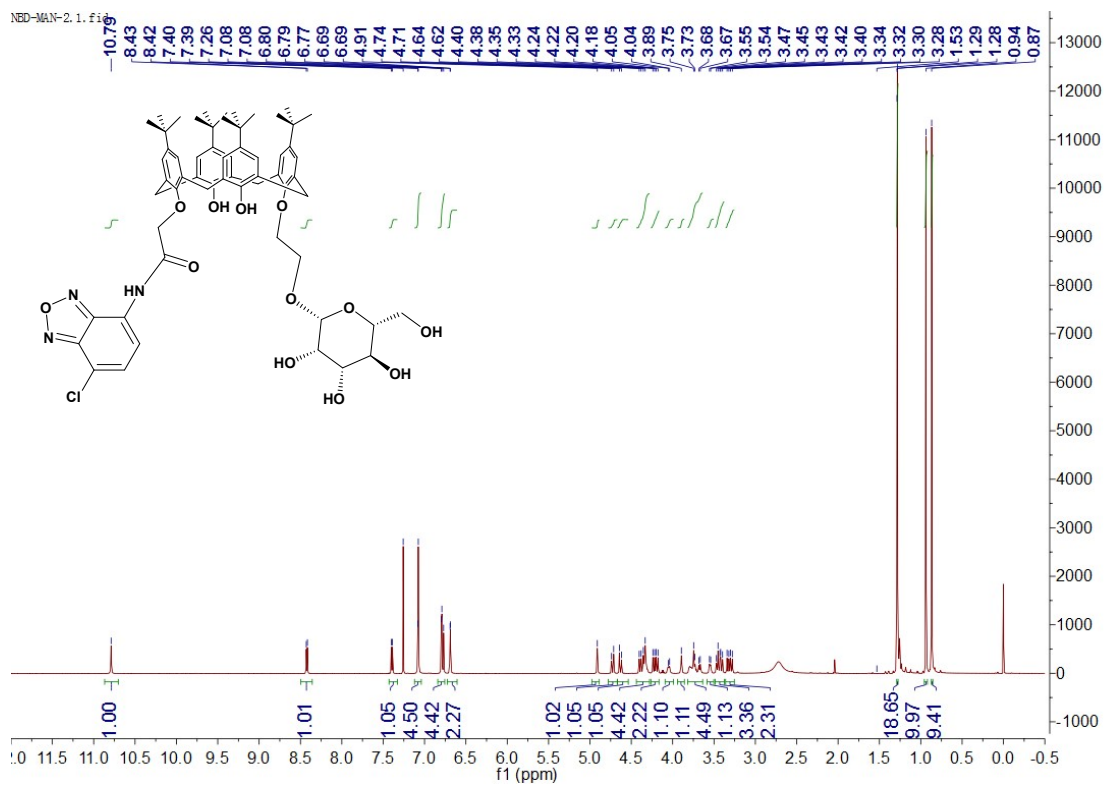


Figure S6. $^1\text{H-NMR}$ (600 MHz) spectrum of NBD-Man-CA in CDCl_3 .

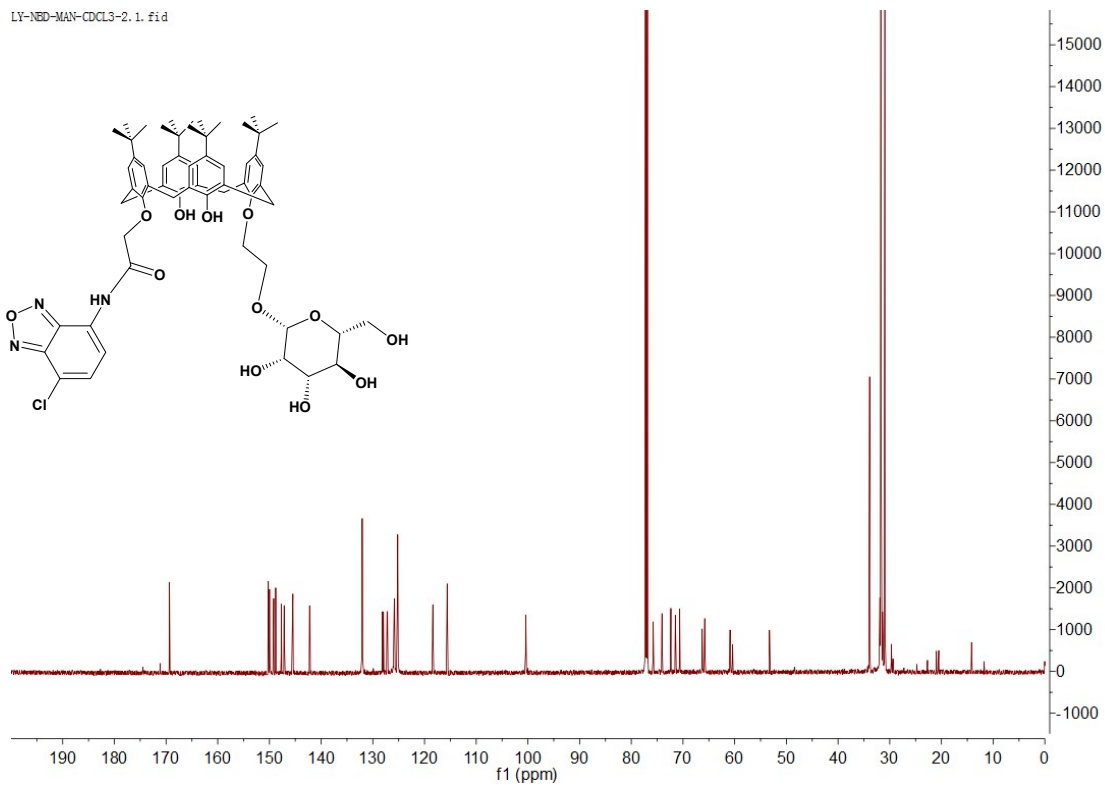


Figure S7. $^{13}\text{C-NMR}$ (150 MHz) spectrum of NBD-Man-CA in CDCl_3 .

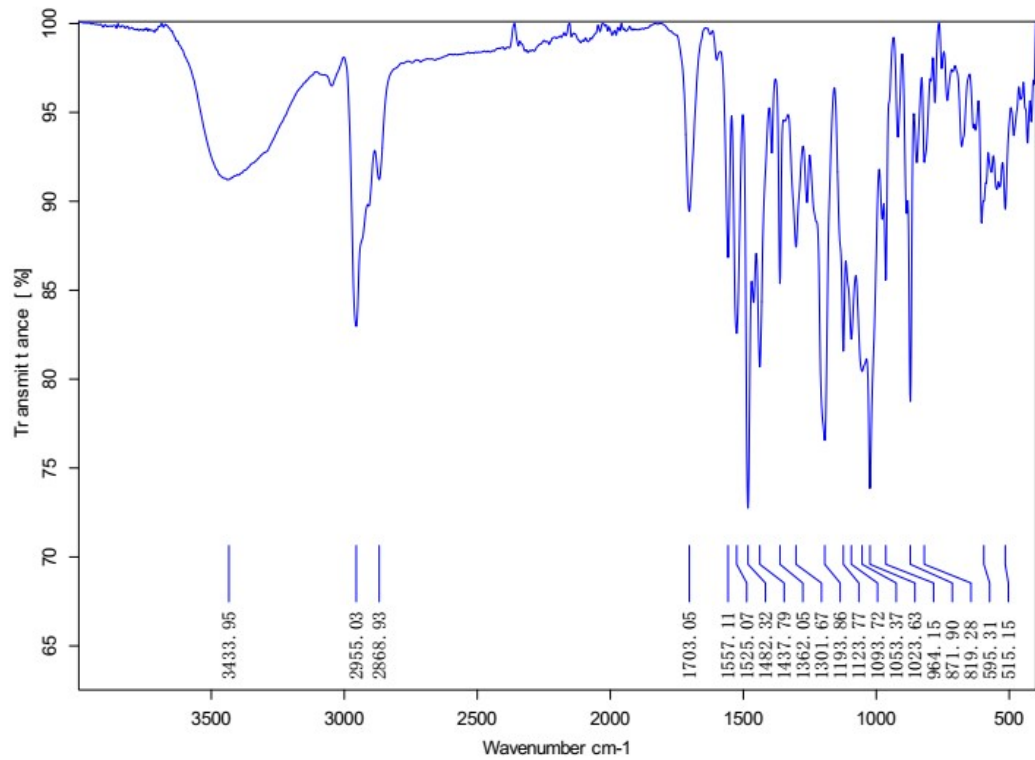


Figure S8. IR spectrum of compound NBD-Man-CA.

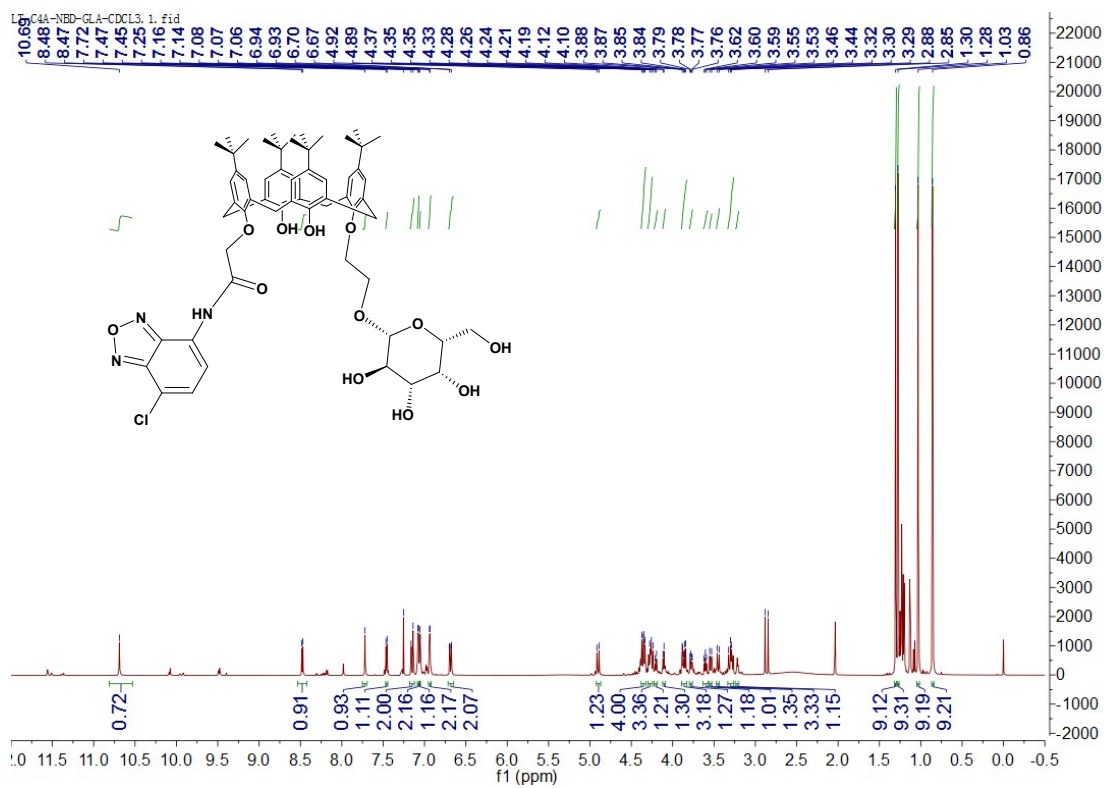


Figure S9. $^1\text{H-NMR}$ (600 MHz) spectrum of NBD-Gal-CA in CDCl_3 .

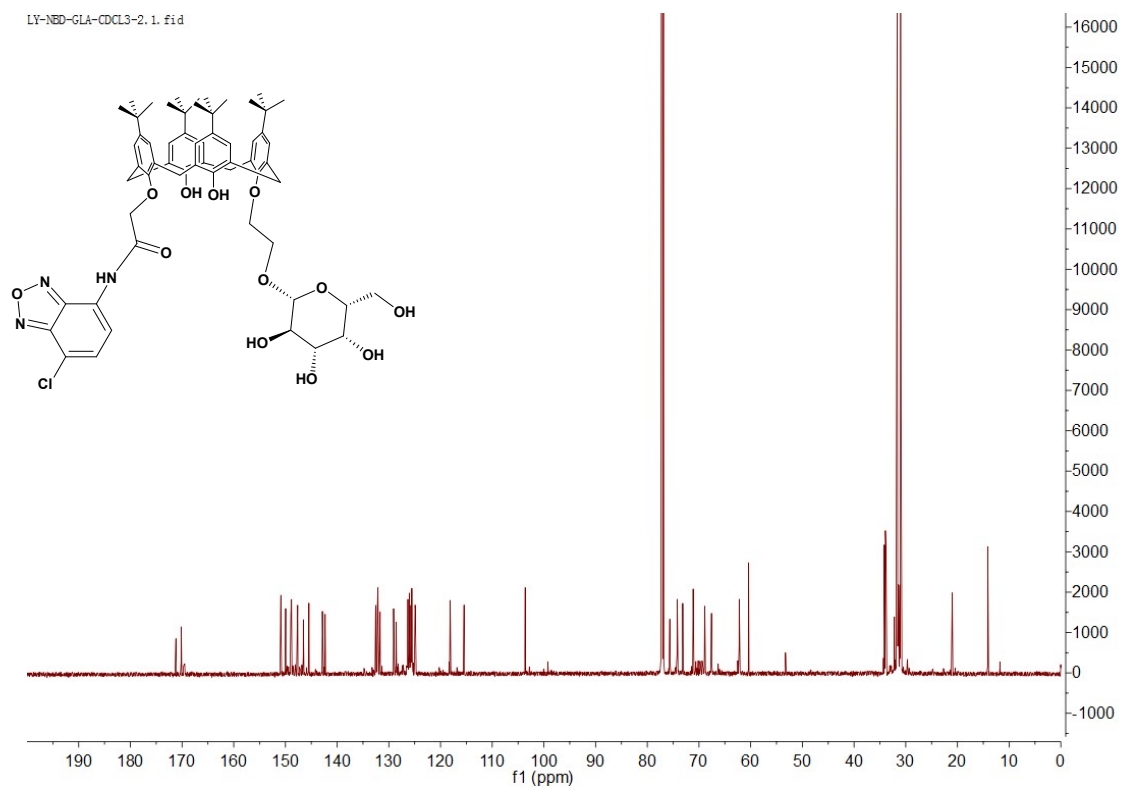


Figure S10. ^{13}C -NMR (150 MHz) spectrum of NBD-Gal-CA in CDCl_3 .

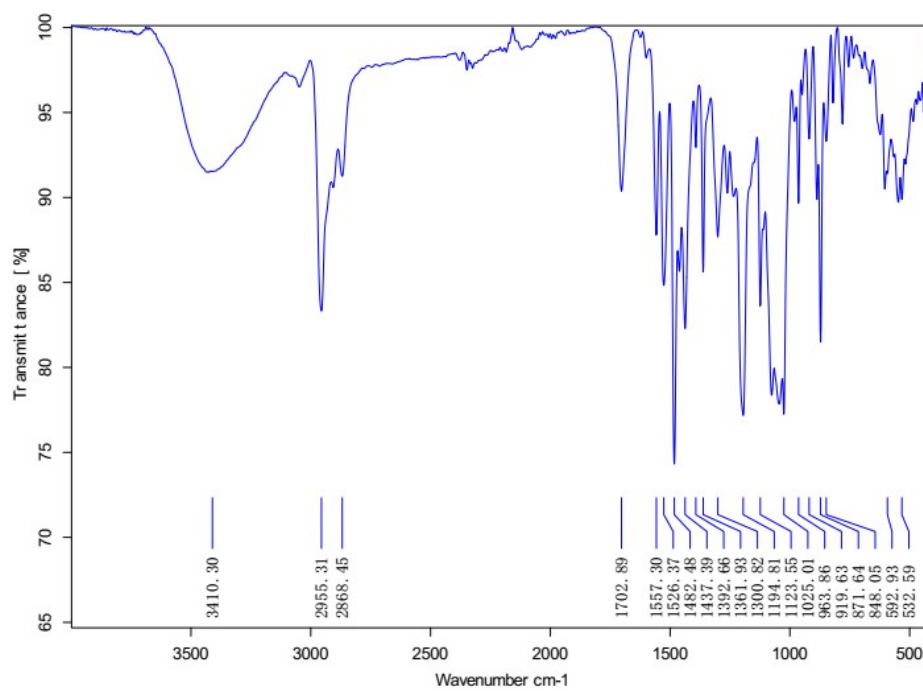


Figure S11. IR spectrum of NBD-Gal-CA.

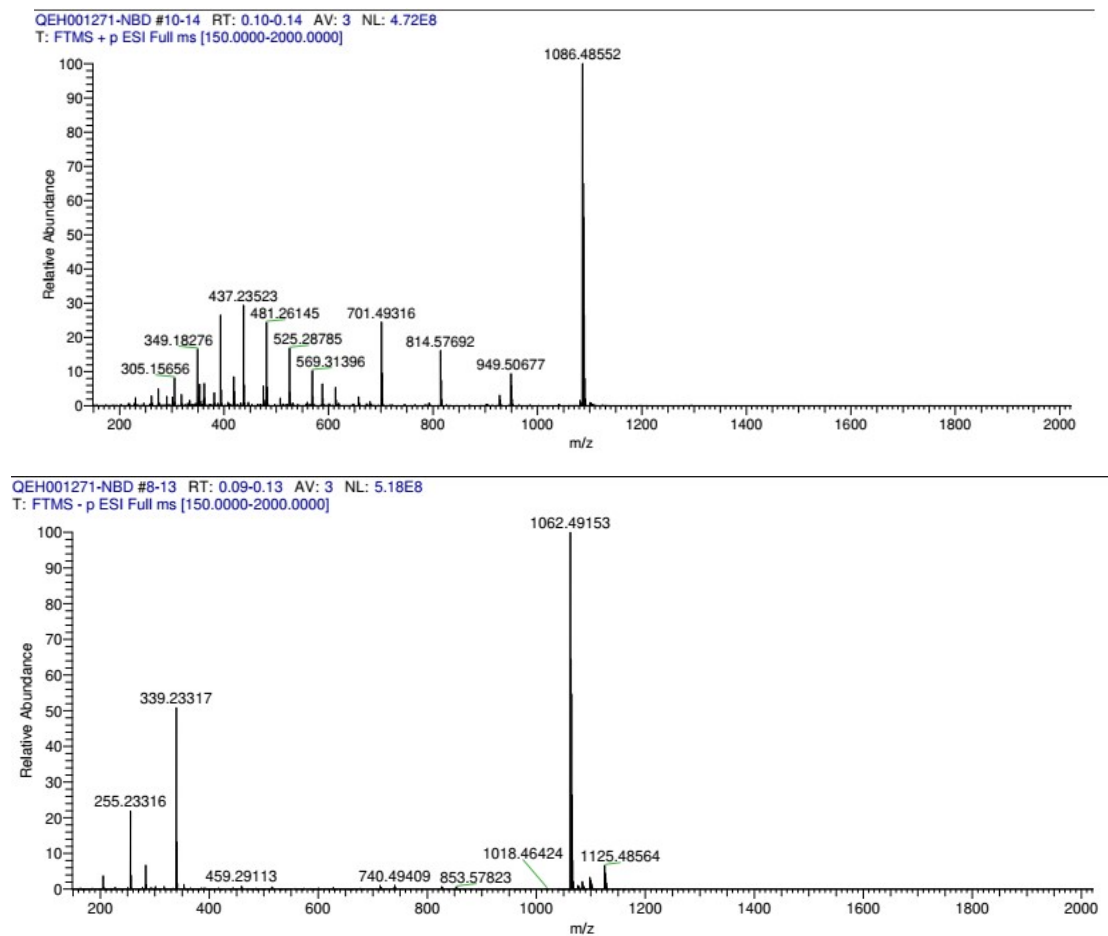


Figure S12. HRMS spectrum of NBD-Gal-CA.

4. Photophysical Properties of the Probes

UV-visible and Fluorescence Spectroscopy. The UV-visible spectroscopic analysis and fluorescence spectroscopic studies were performed by using a Varioskan LUX multimode microplate reader (Thermo Fisher Scientific) to acquire the absorption, excitation and emission spectra of the probe. First, 100 μM stock solutions of NBD-Gly-CA DMSO (Tokyo Chemical Industry) were prepared by vortexing followed by ultrasonication for 15 min and were shaken by hand during the ultrasound treatment. The stock solution was further diluted with PBS to 10 μM working solutions. A 96-well black polystyrene microplate (Thermo Fisher) was used for fluorescence measurements in the ranges of $\lambda_{\text{ex}} = 200\text{--}450$ and $\lambda_{\text{em}} = 300\text{--}700$ nm.

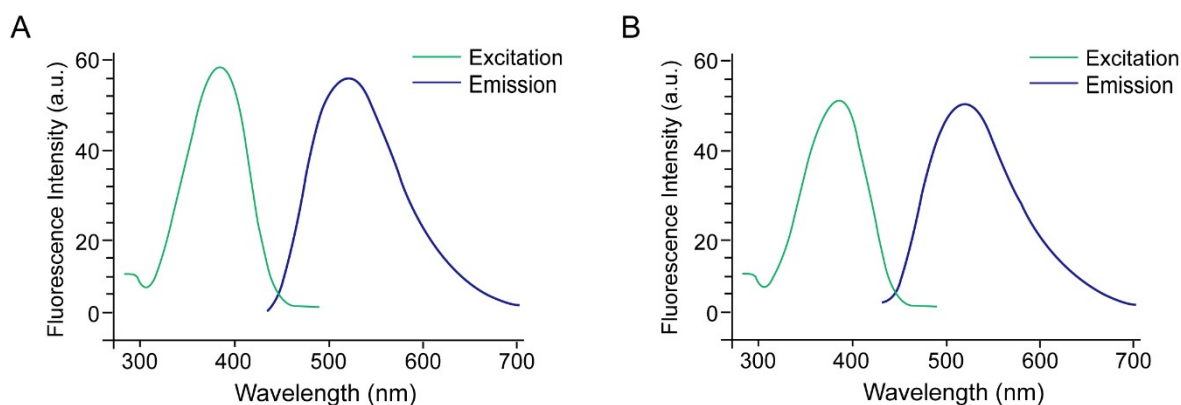


Figure S13. Fluorescent spectrum of NBD-Gly-CA. (A) Fluorescent spectrum of NBD-Glc-CA. (B) Fluorescent spectrum of NBD-Gal-CA. 10 μM of NBD-Gly-CA in DMSO at r.t.

5. Biology Experimental Procedures

Cell lines and Cell Culture. Human bronchial epithelium cell BEAS-2B, human non-small-cell lung cancer cell A549 and human mammary epithelial cell line MCF10A were purchased from ATCC. Human triple negative breast cancer cells MDA-MB-468 was a gift from Tianjin Medical University Cancer Institute & Hospital. A549 cells were cultured at 37°C in RPMI 1640 medium (High Glucose; Gibco, Invitrogen), and supplemented with 10% fetal bovine serum (FBS; Gibco, Invitrogen) and 1% penicillin/streptomycin solution (Gibco, Invitrogen) in humidified atmosphere with 5% CO₂. BEAS-2B, MCF-10A and MDA-MB-468 cells were cultured in Dulbecco's modified Eagle's medium (DMEM 1x, High Glucose; Gibco, Invitrogen) at 37°C with 10% fetal bovine serum and 100 U.mL⁻¹ penicillin-streptomycin under a 5% CO₂ environment.

Cell Viability Assay. The BEAS-2B, A549, MCF-10A and MDA-MB-468 cells were seeded at a density of 5,000 cells per well in a flat bottomed 96-well using 100 μL of culture medium on day 0. On day one, cells were treated with increasing doses of NBD-Gly-CA for 72h, keeping a final concentration of 0.5% DMSO. 100 μL of culture medium was removed. MTT (Sigma-Aldrich) was added to each well at the final concentration of 0.83 mg/mL and incubated for 4 h. Cells were lysed by MTT lysis buffer (15% SDS, 0.015MHCl) and the uptake of MTT was measured at 490 nm using a multi-well-reading UV-Vis spectrometer. For each compound, cell survival rates were expressed as the relative percentage of absorbance compared to controls without drug. Experiments were performed in four replicates (4 wells of the 96-well plate per experimental condition) and repeated for three times.

NBD-Gly-CA accumulation in different cell lines. The spectroscopic evaluation was conducted in PBS at pH 7.4 by using a Thermo Scientific Varioskan LUX multimode microplate reader. As shown in Fig. S14 and as has been reported previously,^[1]

ATP-mediated glucose uptake inhibition. For ATP measurement, a commercially available

luciferin-luciferase assay kit was used. Follow the assay protocol, L929 cells were seeded into 96-well plates using glucose and serum free culture medium to starve cells overnight. Then cells were treated with various concentrations of NBD-Man-CA for 2 h. Then the cells were incubated with 80 μ L of PBS containing 1 μ M of rotenone and 1 mM of glucose. Rotenone (1 μ M) only treated wells were used as negative control, rotenone (1 μ M) with glucose (1 mM) was used as positive control. After a single wash with ice-cold PBS, 100 μ L of CTL buffer (CellTiter-Lumi™ Luminescent Cell Viability Assay Kit, Beyotime) was added, vibrated with a shaker for 2 min, and incubated at 37 °C for 10 min. Finally, loading the plate into the microplate reader and perform luminescence measurement

Confocal Imaging Analysis. Testing cells were aliquoted into 6-well plates. Confocal experiments were started by the addition of 500 nM of NBD-Man-CA into each sample. After 30 min of incubation at 37 °C, the cells were washed 3 times with cold PBS and seeded in glass bottom dish (NEST, China). The chamber slides were then mounted and sealed for confocal microscopic analysis using an Olympus FV1000-IX81 confocal-laser scanning microscope with 488 nm excitation through a 100 \times 1.4 NA oil immersion objective lens.

In Vivo Fluorescence Imaging of NBD-Man-CA in MDA-MB-468 Xenograft Mice. For *In vivo* studies, all experiments were performed according to the regulation and guideline of Institutional Animal Care and Use Committee at Tianjin Medical University Cancer Institute and Hospital by following the Guide for the Care and Use of Laboratory Animals (NRC 2011).

Four to six week-old athymic female nude mice (from Beijing Vital River Laboratory Animal Technology Co., Ltd.) were subcutaneously inoculated with MDA-MB-468 cells (8×10^6) at right flank region next to the hindlimb. When tumor sizes reach 5-10 mm-diameter, 200 μ L of 0.53 mg/mL NBD-Man-CA (0.1 μ mol, 0.11 mg/mice) was administered by tail intravenous injection. Fluorescence imaging was performed with a Xenogen IVIS small animal imaging system and the images were captured by a low noise CCD camera. After completion of the experiment, the nude mice were sacrificed and the main organs as well as tumors were harvested. The fluorescence images of these organs were individually taken as above. Assessment of the tumor-to-background ratio, ovoid regions of interest (ROI) were manually selected over the tumors to measure the fluorescence intensity of tumor (FI_{tumor}), a second ROI was drawn on the contralateral site as background control (FI_{bkg}). Tumor-to-background ratio were calculated based on the following formula:

$$\text{Tumor-to-background ratio (Tm/Bkg)} = FI_{\text{tumor}} / FI_{\text{bkg}}$$

The tumor-to-organ ratio for groups of mice (n=3) was based on the *ex-vivo* optical imaging results of the tumor and selected organs. Average fluorescence intensity of the selected organs (FI_{org}) was used in the following formula:

$$\text{Tumor-to-organ ratio (Tm/Org)} = FI_{\text{tumor}} / FI_{\text{org}}$$

6. Biological Assay Results

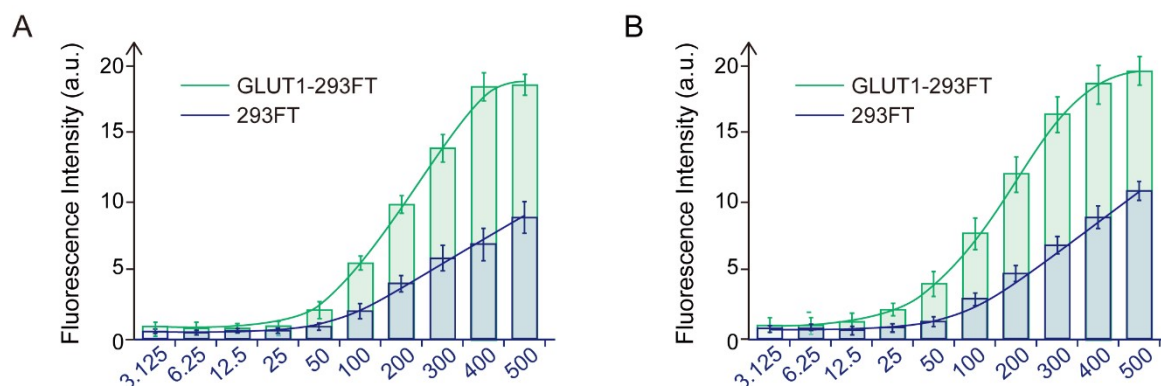


Figure S14. NBD-Gly-CA accumulation in different cell lines. (A) Concentration dependent (3.125-500 μM) cellular uptake of NBD-Glc-CA in GLUT1-293FT and 293FT cells. (B) Concentration dependent (3.125-500 μM) cellular uptake of NBD-Gal-CA in GLUT1-293FT and 293FT cells.

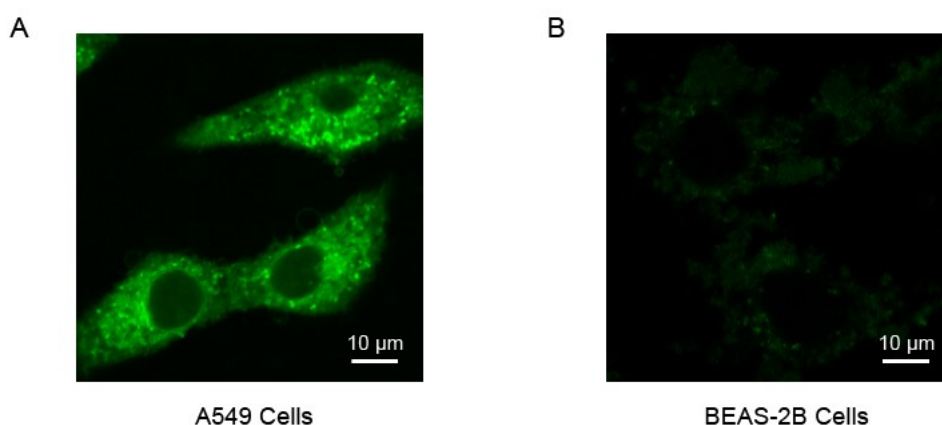


Figure S15. Confocal fluorescence microscopy imaging of NBD-Man-CA in different cell lines. (A) Confocal fluorescence microscopy imaging of A549 cells treated with 500 nM of NBD-Man-CA at 37 °C incubated for 30 min. (B) Confocal fluorescence microscopy imaging of BEAS-2B cells treated with 500 nM of NBD-Man-CA at 37 °C incubated for 30 min.

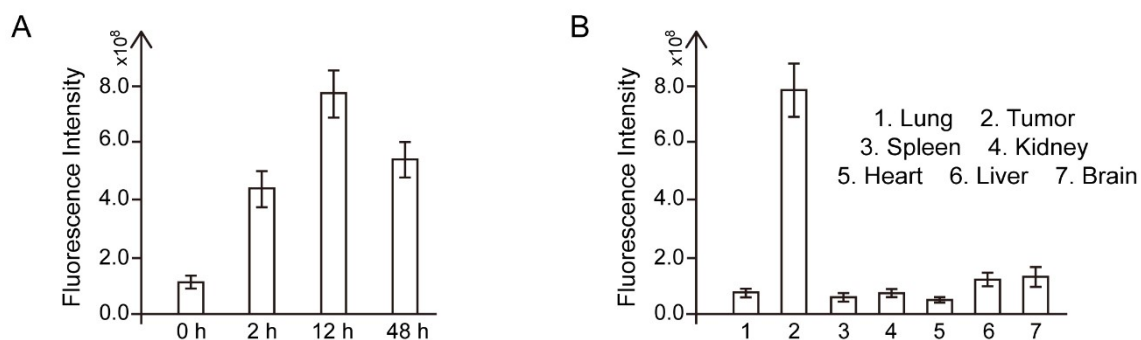


Fig. S16. In vivo imaging for NBD-Man-CA treated MDA-MB-468 xenograft mice. (A) Quantitative analysis of mean fluorescence intensity of NBD-Man-CA determined over time by measurement of respective tumor

regions of interest, (averaged from n=3). (B) The quantitative biodistribution of NBD-Man-CA from *ex vivo* tumor tissues and organs (n=3, at 48 h). λ_{ex} . 470 ± 10 nm and λ_{em} . 565 ± 20 nm.

Table S1. Tumor-to-background ration (Tm/Bkg) and tumot-to-organ ratio (Tm/Org) for NBD-Man-CA treated MDA-MB-468 bearing xenograft mice.

□ NBD-Man-CA Treated MDA-MB-468 Xenograft Mice			
Time	2 h	12 h	48 h
Tm/Bkg ^a	3.9595	6.9614	4.8714
Tm/Org ^b	□9.2237 (at 48 h)		

^a Based on fluorescence intensity of tumor (FI_{tumor}) and background ((FI_{bkg})) measured from living animals for each time point. ^b Based on average fluorescence intensity of tumor (FI_{tumor}) and of the selected organs (FI_{org}) measured from *ex vivo* samples (n=3).

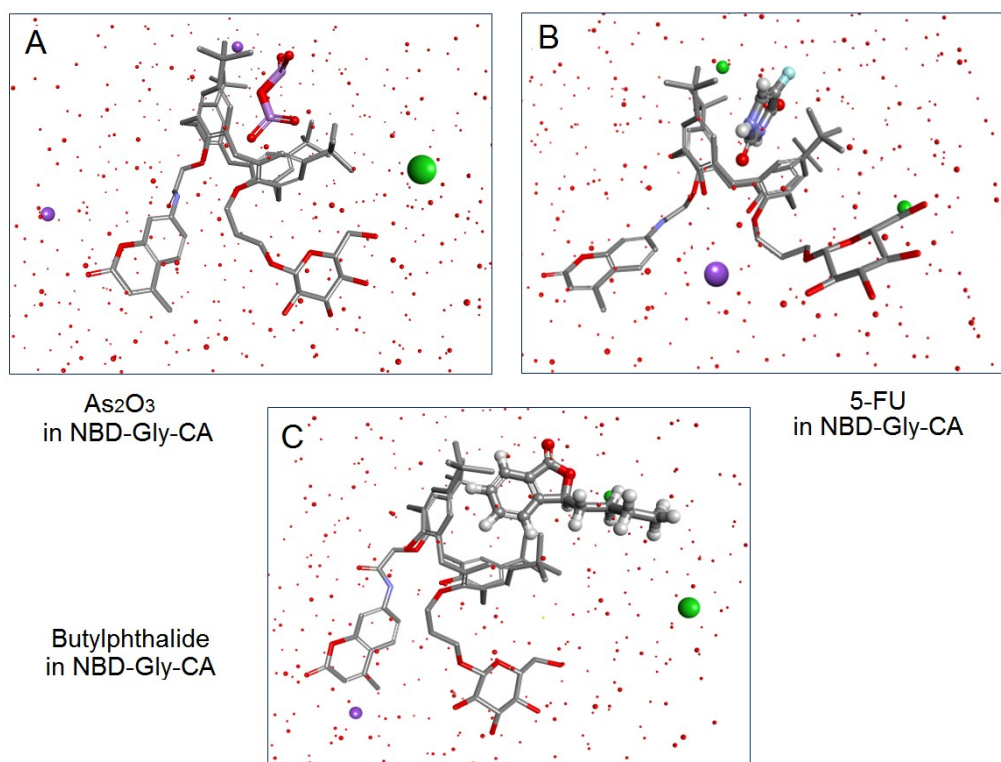


Figure S17. Molecular dynamics simulations of NBD-Gly-CA with different drug molecules in a fully solvated physiological conditions. (A) Molecular dynamics simulations result of NBD-Man-CA with Arsenic trioxide. (B) MD simulation result of NBD-Man-CA with 5-FU. (C) MD simulation result of NBD-Man-CA with butylphthalide. (YASARA dynamics software was used, solvation with 0.9% NaCl, 298 K, pH 7.4. Green sphere = Cl⁻, Purple sphere = Na⁺).

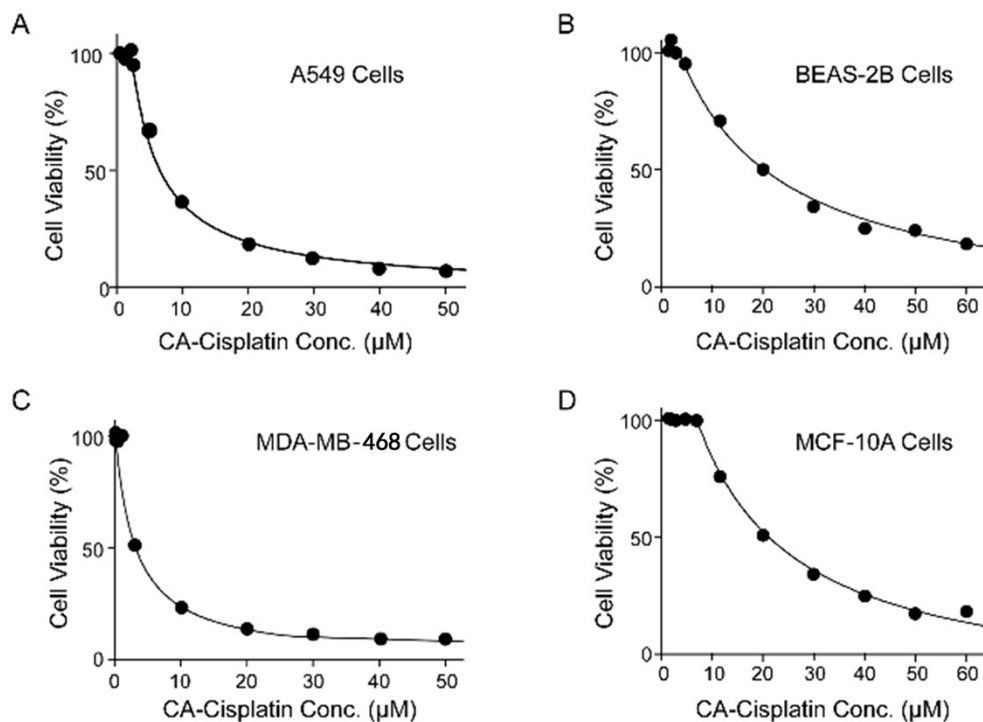


Figure S18. *In vitro* cytotoxicities of DDP-NBD-Man-CA against (A) A549 cells (B) BEAS-2B cells, (C) MDA-MB-468 cells, and (D) MCF-10A cells respectively after 72 h incubation.

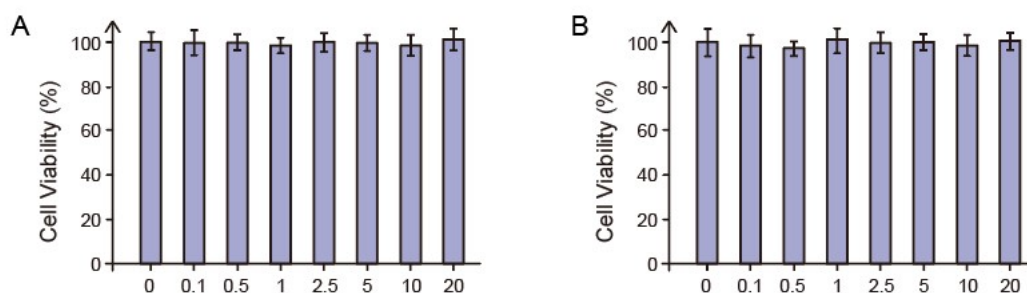


Figure S19. Cytotoxicity of NBD-Gly-CA in A549 and MDA-MB-468 cells. (A) 72 h cytotoxicity results for NBD-Man-CA in A549 cells from MTT assay. (B) 72 h cytotoxicity results for NBD-Man-CA in DA-MB-468 cells from MTT assay. Data were presented as mean \pm S.E.M.

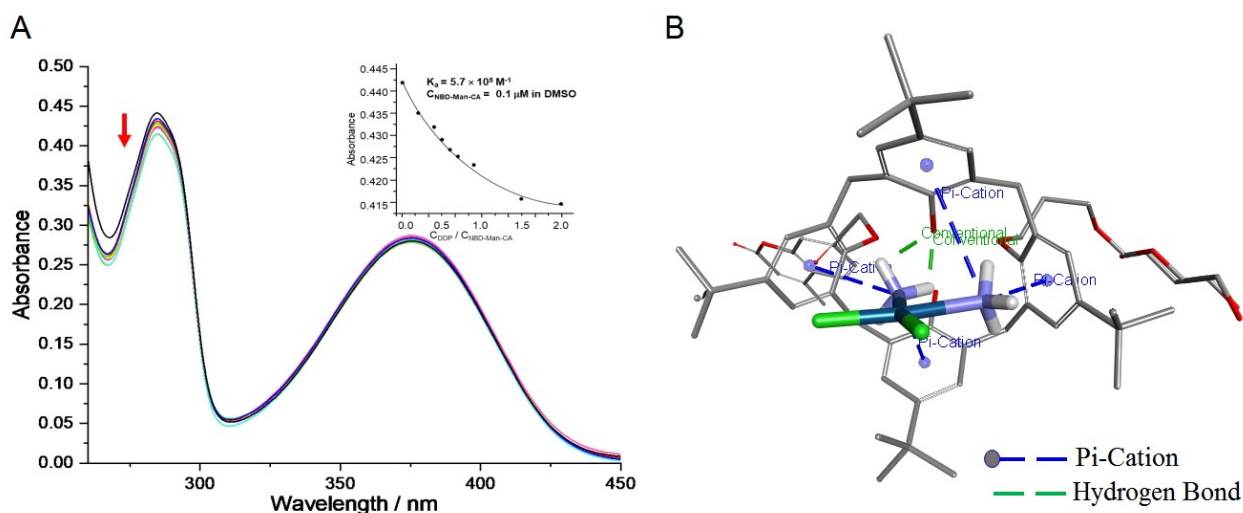


Figure S20. Binding constant of DDP⊂NBD-Man-CA and hypothesized host-guest interactions. (A) UV-vis spectra of NBD-Man-CA at a fixed concentration of 0.1 μM in DMSO with different concentrations of DDP (μM): 0.00 to 0.20. Inset: the nonlinear regression by plotting the change in absorbance versus concentration ratio of DDP/NBD-Man-CA that were analyzed by nonlinear least-squares method using an equation for 1:1 binding model. UV-visible spectroscopic analysis was performed using a U-3900 UV-VIS spectrophotometer at 25 $^{\circ}\text{C}$ with a quartz cuvette having a pathlength of 0.2 cm as a sample holder. (B) Illustration of the binding interactions between DDP and NBD-Man-CA from the molecular docking result.

References

- [1] S. Liu, W. Song, Y. Cui, Z. Sun, et al., *Chem. Commun.*, 2021, **57**, 5530.